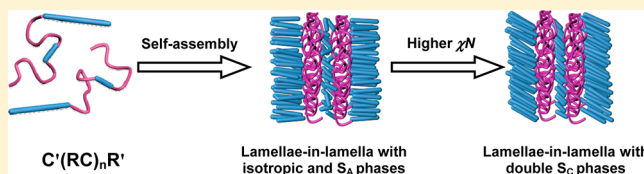


Self-Assembly of Rod–Coil Multiblock Copolymers: A Strategy for Creating Hierarchical Smectic Structures

Xiaomeng Zhu, Liquan Wang, and Jiaping Lin*

Shanghai Key Laboratory of Advanced Polymeric Materials, Key Laboratory for Ultrafine Materials of Ministry of Education, School of Materials Science and Engineering, East China University of Science and Technology, Shanghai 200237, China

ABSTRACT: We extended self-consistent field theory to explore self-assembly behavior of linear multiblock copolymers consisting of alternative rod and coil blocks. Such rod–coil multiblock copolymers are found to be capable of self-assembling into hierarchical smectic microstructures. For the copolymers with long rod end block, lamellae-in-lamellar structures containing two smectic C phases at small and large length scales were observed. It was found that the hierarchical smectic structures exhibit not only double periodicities in overall structure but also double orientational orders of rod blocks. Additionally, these hierarchical smectic structures can be tailored by tuning the relative length of the coil blocks. For the copolymers with long coil end block, the multiblock copolymers can self-assemble into hierarchical lamellar structures with smectic phases only at the small length scale. The findings gained through the present study may offer valuable information for understanding the self-assembly behavior of complicated rod–coil copolymers and designing polymeric materials with advanced properties.



INTRODUCTION

Materials with highly ordered and sophisticated microstructures usually exhibit more advanced macroscopic properties than those with traditional lamellar or cylindrical structures. Such special structures can be created by the self-assembly of diverse polymer systems. So far, a lot of macromolecules with designed shapes or topologies have been synthesized and have attracted increasing attention for their promising applications in fabricating advanced functional materials with sophisticated microstructures.^{1–8} A typical example is provided by rod–coil type copolymers which are able to self-assemble into various microstructures with liquid crystalline (LC) phases. The microstructures formed from the rod–coil copolymers have two characteristics, i.e., orientational ordering of rodlike units and morphological organization of immiscible rod/coil chains (Figure 1a).^{9–11} Inspired by these structural characteristics of LC structures, a variety of complex LC microstructures have been designed and produced by the rod–coil copolymers. They include rectangular columnar phase, oblique columnar phase, and tetragonal mesophase, etc.² Specially, main- or side-chain rod–coil copolymers have been considered as the ideal model systems for building these LC structures.^{12–16} Although these microstructures are sophisticated, they possess only one structural period at the nanoscale.

Recently, hierarchical nanostructures which possess multiple periods at different length scales have received considerable attentions. For example, ten Brinke et al. reported that supramolecular comb–coil block copolymers with low-molecular-weight compound linked to the block copolymer chains are capable of self-organizing into structure-in-structure morphologies.^{17–20} These hierarchical structures have double periodicities, including the large period of diblock copolymers and the small period of comb-shaped blocks. In addition,

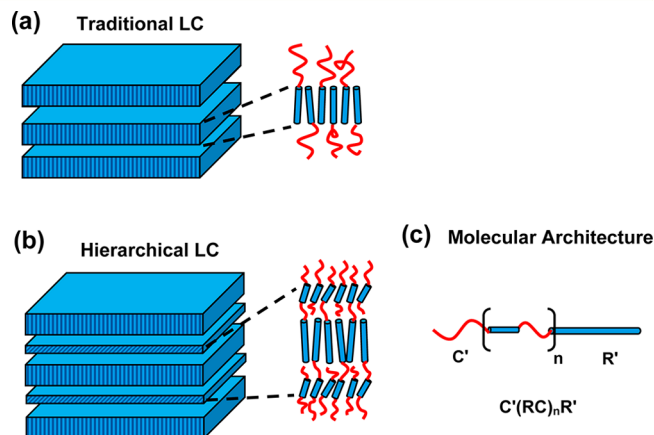


Figure 1. Schematic representation of (a) a traditional LC structure and (b) a hierarchical LC structure. The mesogenic units (blue) align perpendicular to the LC layers which are alternated with amorphous regions of coil blocks (red). (c) Molecular architecture of $C'(RC)_nR'$ rod–coil multiblock copolymer.

Matsushita et al. synthesized a series of linear multiblock copolymers such as $V(IS)_nIV$ and $V(IS)_nI$, where V, I, and S refer to poly(2-vinylpyridine), poly(isoprene), and poly(styrene), respectively.^{21–24} Such copolymers can also self-assemble into various structure-in-structures, e.g., onionlike sphere and coaxial cylinder, with two different length scales. Combining the concepts of hierarchical microstructures with LC phases, a different class of hierarchical structures can be anticipated, that is,

Received: January 25, 2013

Revised: April 1, 2013

Published: April 12, 2013

hierarchical liquid crystalline structures which show multiscale spatial orders over both LC and amorphous domains, such as amorphous lamellae separated by double smectic layers (Figure 1b). These structures show obvious difference from the traditional LC structures. Soft materials with such hierarchical LC structures could bring a significant advance in areas including electrooptical devices, high modulus fibers, and biosystems.^{25–29}

Several recent experiments have been focused on this type of hierarchical LC structures, by introducing two kinds of chemically different liquid crystalline molecules into the systems.^{30–32} Different from such a strategy, copolymers with only one kind of liquid crystalline polymer but various lengths of the blocks are also capable of forming the hierarchical LC structures. For example, linear $C'(RC)_nR'$ multiblock copolymers containing long molecular “tails” and a repeating multiblock group are one of the promising molecular models for constructing the hierarchical LC structures, as shown in Figure 1c (R and C represent the rod and coil blocks, and the prime denotes the end blocks). The design of such a molecular architecture is originated from that of flexible multiblock copolymer systems. Because of the large parameter space that characterizes the rod–coil multiblock copolymers, the experimental exploration could be a very costly and time-consuming task. From this perspective, theory and simulation provide an alternative tool for exploring the self-assembly behaviors of rod–coil block copolymer systems. Some simulation studies on the self-assembly of simple rod–coil copolymers have already been reported.^{33–40} For example, Matsen and Barrett have used the self-consistent field theory (SCFT) in Semenov–Vasilenko model to examine the phase behavior of rod–coil diblock copolymers.³³ It was found that the behaviors are mainly controlled by the rod/coil interactions, the volume fraction of coil blocks, and the length ratio of the coil to rod blocks. Nematic phase is stable when $\chi N \leq S$, and various smectic phases appear with increasing χN . Additionally, Pryamitsyn and Ganesan performed 1D and 2D SCFT studies on such rod–coil block copolymers, with the Maier–Saupe model for the orientational interactions between the rod blocks.^{34–36} Several nonlamellar phases, such as broken lamellar phases, arrowhead phases, and smectic C phases, were observed. These phases have been observed in the experiments. The SCFT was also commonly used for wormlike chain model.^{37,38} Shah and Ganesan investigated the chain bridging in lamellae of linear multiblock copolymers.³⁸ They found that the bridging conformation in crystalline domain increases with an increase in the rigidity of the semiflexible blocks. Moreover, An et al. proposed a novel SCFT lattice model for probing the microstructures.^{39,40} Micellar, perforated lamellar, gyroid, and zigzag phases have been obtained with a random initial assumption of structures. The orientation of rod blocks can also be evaluated by their new approaches. The success of the SCFT simulations in rod–coil systems motivates our interest in predicting the hierarchical structures of rod–coil multiblock copolymers.

In previous works, we found that various copolymer systems (e.g., $A(BC)_n$ multiblock copolymer) can self-assemble into hierarchically ordered nanostructures, such as lamellae-in-lamella, cylinders-in-lamella, cylinders-in-cylinder, and spheres-in-sphere.^{41–43} Herein, we extended the real-space SCFT with the model proposed by Pryamitsyn and Ganesan to investigate the hierarchical self-assembly behaviors of $C'(RC)_nR'$ multiblock copolymers.³⁶ A series of smectic-in-smectic, isotropic-in-smectic, and smectic-in-amorphous phases were discovered. It was found

that the length of rod blocks plays an important role in the formation of such hierarchical structures. The influences of interaction strength on the orientational ordering of the rod blocks at different length scales were also investigated. Furthermore, the length of coil blocks was found to have marked effect on the hierarchical structures. For the $C'(RC)_nR'$ multiblock copolymers with long coil end block, hierarchical structures with only one smectic phase at the small length scale can be obtained. We expect that the present work could provide useful information for understanding the self-assembly behavior of rod–coil multiblock copolymers.

METHODS

We considered the system with volume V containing $C'(RC)_nR'$ rod–coil multiblock copolymers. Each copolymer consists of two different end blocks (C' and R') connected to a $(RC)_n$ multiblock composed of n repeating units of the elementary RC diblock. We denoted C and R as coil and rod blocks, respectively, as schematically illustrated in Figure 1c. The copolymers are considered to be monodisperse. The total volume fractions of rod and coil blocks are $1 - f$ and f , respectively. Each coil block is scaled as a statistical segment length a , and the rod blocks have a segment length b . We defined that the volume of each segment (coil and rod) is ρ_0^{-1} . The total degree of polymerization of the multiblock copolymer is $N \equiv N_{C'} + n(N_C + N_R) + N_{R'}$, where $N_{C'}$, N_C , N_R , and $N_{R'}$ denote the length of coil and rod blocks (the prime symbol represents the blocks at the end). Accordingly, the volume fractions of each block are specified as $f_{C'(R')} = N_{C'(R')}/N$ and $\Delta f_{C(R)} = N_{C(R)}/nN$.

In the present work, the SCFT model of Pryamitsyn and Ganesan was extended to involve rod–coil multiple blocks.^{36,44} Herein, we consider the configurations of a single copolymer chain in a set of effective chemical potential field $\omega_i(\mathbf{r})$, where i denotes block species C and R. The incompressibility ($\varphi_C(\mathbf{r}) + \varphi_R(\mathbf{r}) = 1$) has been invoked by introducing a Lagrange multiplier $\xi(\mathbf{r})$. The free energy per chain can be written as (in units of $k_B T$)

$$F = -\ln\left(\frac{Q}{V}\right) + \frac{1}{V} \int d\mathbf{r} \left\{ \chi N \varphi_R(\mathbf{r}) \varphi_C(\mathbf{r}) - \sum_{I=R,C} \omega_I(\mathbf{r}) \varphi_I(\mathbf{r}) - \xi(\mathbf{r}) \left(1 - \sum_{I=R,C} \varphi_I(\mathbf{r}) \right) + \mathbf{M}(\mathbf{r}) : \mathbf{S}(\mathbf{r}) - \frac{\mu N}{2} \mathbf{S}(\mathbf{r}) : \mathbf{S}(\mathbf{r}) \right\} \quad (1)$$

where χ is the Flory–Huggins parameter between different species C and R and μ is the Maier–Saupe orientational interaction describing the alignment of the rods. Q is the partition function of a single chain in the effective chemical potential field $\omega_i(\mathbf{r})$ ($i = R, C$) and the conjugated tensorial orientation field $\mathbf{M}(\mathbf{r})$, which involves the terms of propagators $q(\mathbf{r}, s)$ and $q^\dagger(\mathbf{r}, s)$. The spatial coordinate \mathbf{r} is rescaled by R_g , where $R_g^2 = a^2 N / 6$. The contour length is parametrized with variable s , which starts from coil end ($s = 0$) to the rod end ($s = 1$). The propagators $q(\mathbf{r}, s)$, according to a flexible Gaussian chain model, satisfy the following modified diffusion equations ($0 \leq i < n$)

$$\begin{aligned}\frac{\partial q(\mathbf{r}, s)}{\partial s} &= [R_g^2 \nabla^2 - \omega_C(\mathbf{r})] q(\mathbf{r}, s) \\ -\frac{\partial q^\dagger(\mathbf{r}, s)}{\partial s} &= [R_g^2 \nabla^2 - \omega_C(\mathbf{r})] q^\dagger(\mathbf{r}, s) \\ (0 \leq s < f_{C'}, f_{C'} + i(\Delta f_R + \Delta f_C) + \Delta f_R \\ &\leq s < f_{C'} + (i+1)(\Delta f_R + \Delta f_C))\end{aligned}\quad (2)$$

with the initial conditions $q(\mathbf{r}, 0) = 1$ and $q^\dagger(\mathbf{r}, 1 - f_{R'}) = \int d\mathbf{u} \exp[-\int_0^{f_{R'}} ds \Gamma(\mathbf{r} + \beta s \mathbf{u}, \mathbf{u})]$, where \mathbf{u} is a unit vector characterizing the orientation of rods in the s th segment and β is the size asymmetry ratio, that is, $\beta = 6^{1/2} \nu^{-1}$ ($\nu = aN^{1/2}/bN$). $\Gamma(\mathbf{r}, \mathbf{u})$ is defined by

$$\Gamma(\mathbf{r}, \mathbf{u}) \equiv \omega_R(\mathbf{r}) - \mathbf{M}(\mathbf{r}) : \left(\mathbf{u} \mathbf{u} - \frac{\mathbf{I}}{3} \right) \quad (3)$$

where \mathbf{I} is a 3×3 identical matrix. Similarly, the propagators of each rod-coil junctions are given by

$$\begin{aligned}q(\mathbf{r}, f_{C'} + i(\Delta f_R + \Delta f_C) + \Delta f_R) &= q(\mathbf{r}, f_{C'} + i(\Delta f_R + \Delta f_C)) \\ &\times \int d\mathbf{u} \exp[-\int_0^{\Delta f_R} ds \Gamma(\mathbf{r} + \beta s \mathbf{u}, \mathbf{u})]\end{aligned}\quad (4)$$

$$\begin{aligned}q^\dagger(\mathbf{r}, f_{C'} + i(\Delta f_R + \Delta f_C)) &= q^\dagger(\mathbf{r}, f_{C'} + i(\Delta f_R + \Delta f_C) + \Delta f_R) \\ &\times \int d\mathbf{u} \exp[-\int_0^{\Delta f_R} ds \Gamma(\mathbf{r} + \beta s \mathbf{u}, \mathbf{u})]\end{aligned}\quad (5)$$

The partition function Q for an unconstrained chain can be evaluated in terms of the chain propagator $q(\mathbf{r}, s)$:

$$Q = \int d\mathbf{u} \int d\mathbf{r} \exp[-\int_0^{f_{R'}} ds \Gamma(\mathbf{r} + \beta s \mathbf{u}, \mathbf{u})] q(\mathbf{r}, 1 - f_{R'}) \quad (6)$$

Furthermore, the average volume of each block must equal the volume fraction of corresponding block, and the segment densities $\varphi_C(\mathbf{r})$ and $\varphi_R(\mathbf{r})$ along with the orientational order parameter $\mathbf{S}(\mathbf{r})$ follow that

$$\begin{aligned}\varphi_C(\mathbf{r}) &= \frac{V}{Q} \left\{ \int_0^{f_{C'}} ds q(\mathbf{r}, s) q^\dagger(\mathbf{r}, s) \right. \\ &+ \sum_{i=0}^{n-1} \int_{f_{C'} + i(\Delta f_R + \Delta f_C)}^{f_{C'} + (i+1)(\Delta f_R + \Delta f_C)} ds q(\mathbf{r}, s) q^\dagger(\mathbf{r}, s) \left. \right\}\end{aligned}\quad (7)$$

$$\begin{aligned}\varphi_R(\mathbf{r}) &= \frac{V}{Q} \left\{ \int_0^{f_{R'}} ds \int d\mathbf{u} q(\mathbf{r} - \beta s \mathbf{u}, 1 - f_{R'}) \right. \\ &\times \exp[-\int_0^{f_{R'}} ds' \Gamma(\mathbf{r} - \beta s \mathbf{u} + \beta s' \mathbf{u}, \mathbf{u})] \\ &+ \sum_{i=0}^{n-1} \int_0^{\Delta f_R} ds \int d\mathbf{u} q(\mathbf{r} - \beta s \mathbf{u}, f_{C'} + i(\Delta f_R + \Delta f_C)) \\ &\times \exp[-\int_0^{\Delta f_R} ds' \Gamma(\mathbf{r} - \beta s \mathbf{u} + \beta s' \mathbf{u}, \mathbf{u})] \\ &\times q^\dagger(\mathbf{r} + \beta(\Delta f_R - s) \mathbf{u}, f_{C'} + i(\Delta f_R + \Delta f_C) + \Delta f_R) \left. \right\}\end{aligned}\quad (8)$$

$$\begin{aligned}\mathbf{S}(\mathbf{r}) &= \frac{V}{Q} \left\{ \int_0^{f_{R'}} ds \int d\mathbf{u} \left(\mathbf{u} \mathbf{u} - \frac{\mathbf{I}}{3} \right) q(\mathbf{r} - \beta s \mathbf{u}, 1 - f_{R'}) \right. \\ &\times \exp[-\int_0^{f_{R'}} ds' \Gamma(\mathbf{r} - \beta s \mathbf{u} + \beta s' \mathbf{u}, \mathbf{u})] \\ &+ \sum_{i=0}^{n-1} \int_0^{\Delta f_R} ds \int d\mathbf{u} \left(\mathbf{u} \mathbf{u} - \frac{\mathbf{I}}{3} \right) q(\mathbf{r} - \beta s \mathbf{u}, f_{C'} \\ &+ i(\Delta f_R + \Delta f_C)) \exp[-\int_0^{\Delta f_R} ds' \Gamma(\mathbf{r} - \beta s \mathbf{u} + \beta s' \mathbf{u}, \mathbf{u})] \\ &\times q^\dagger(\mathbf{r} + \beta(\Delta f_R - s) \mathbf{u}, f_{C'} + i(\Delta f_R + \Delta f_C) + \Delta f_R) \left. \right\}\end{aligned}\quad (9)$$

Minimization of free energy F , with respect to $\varphi_C(\mathbf{r})$, $\varphi_R(\mathbf{r})$, $\mathbf{S}(\mathbf{r})$, $\omega_C(\mathbf{r})$, $\omega_R(\mathbf{r})$, $\mathbf{M}(\mathbf{r})$, and $\xi(\mathbf{r})$, can lead to a set of mean-field equations:

$$\omega_C(\mathbf{r}) = \chi N \varphi_R(\mathbf{r}) + \xi(\mathbf{r}) \quad (10)$$

$$\omega_R(\mathbf{r}) = \chi N \varphi_C(\mathbf{r}) + \xi(\mathbf{r}) \quad (11)$$

$$\mathbf{M}(\mathbf{r}) = \mu N \mathbf{S}(\mathbf{r}) \quad (12)$$

$$\varphi_R(\mathbf{r}) + \varphi_C(\mathbf{r}) = 1 \quad (13)$$

To numerically solve the SCFT equations, we use a variant of the algorithm developed by Fredrickson and co-workers.^{45–48} The calculations were started from two chosen initial conditions—an initial state with random distribution and oriented configurations and a seeded initial lamellar structure. The diffusion equations were solved via the Baker–Hausdorff operator splitting formula proposed by Rasmussen et al.^{49,50} The densities $\varphi_i(\mathbf{r})$ of species i and order parameter $\mathbf{S}(\mathbf{r})$ of the rods, conjugating respectively the chemical potential fields $\omega_i(\mathbf{r})$ and tensorial orientation fields $\mathbf{M}(\mathbf{r})$, are evaluated with respect to eqs 7–12. The fields $\omega_i(\mathbf{r})$ and $\mathbf{M}(\mathbf{r})$ could be updated by using a two-step Anderson mixing scheme.⁵¹ Our calculations were carried out in one dimension with periodic boundary conditions in z -direction, which leads to a limitation of our results to lamellar structures. To ensure sufficient accuracy of our solution, the spatial resolutions were taken as $\Delta z = 0.1 R_g$. The contour's step size was set as $\Delta s = 0.01$. After testing several contours' step sizes, we found that the free energy in the system can converge to a stable value at these values. The integrals of tilting angle for rod orientation in the equations were evaluated by Gaussian quadrature with 10 points in θ and 20 points in ϕ . The numerical simulation continues until the free energy converges. The box size was optimized by minimizing the free energy of the systems, as suggested by Bohbot-Raviv and Wang.⁵² The stable microstructure was obtained until the global minimum of free energy was achieved.

To obtain the average order parameter $\tilde{\mathbf{S}}$ and the average tilting angle Θ of rods, we first solved the eigenvalue and eigenvector of the average orientational order-parameter tensor $\mathbf{S}(\mathbf{r})$. Then, the order parameter can be obtained as $\tilde{\mathbf{S}} = 3/2 \times \lambda_{\max}$, where λ_{\max} is the largest eigenvalue. Through finding the eigenvector \mathbf{u}_{\max} corresponding to the largest eigenvalue, we can calculate the tilting angle, a angle between vectors \mathbf{u}_{\max} and \mathbf{u}_z of z -axis, as $\cos(\Theta) = \mathbf{u}_{\max} \cdot \mathbf{u}_z$. Note that the tilting angle is an ensemble-average value.

RESULTS AND DISCUSSION

In the present work, we investigated the influence of molecular architecture on the self-assembled hierarchical structures of

$C'(RC)_nR'$ multiblock copolymers. The volume fractions of the rod or coil end block are ranged from 0.4 to 0.6 for constructing domains at large length scales, and the volume fractions of R and C midblocks in (RC) repeat units are set to be equal for creating lamellar substructures at small length scales. According to the work of Pryamitsyn and Ganesan,³⁶ other important parameters in the simulations are chosen as follows. The ν in $\beta = \sqrt{6\nu^{-1}}$ and $G = \mu/\chi$ are fixed as 0.25 and 4, respectively. In addition, the number n of repeat units is selected as 1 or 2.

1. Hierarchical Smectic Structures Self-Assembled from $C'(RC)_nR'$ with Long R' End Block. We first focused on the self-assembly behavior of $C'(RC)_nR'$ multiblock copolymers with a longer R' end block (relative to C' end block). In the self-assembly of these multiblock copolymers, the large-length-scale structures can be generated by microphase separation between the long R' end blocks and remainder $C'(RC)_n$ blocks. In this case, the $C'(RC)_n$ blocks can be regarded as one block and, thus, the phase behavior resembles that of rod-coil diblock copolymer with a long rod end block. As reported by Pryamitsyn and Ganesan, the rod-coil diblock copolymers with large volume fraction of rod block incline to form a series of smectic phases, such as monolayer smectic A (S_A), smectic C (S_C), and bilayer smectic structures.³⁶ As a result, a smectic phase at large length scales could be obtained from the self-assembly of these copolymers. Moreover, the microphase separation of the remainder $C'(RC)_n$ blocks could further produce another liquid crystalline structure at small length scale.

Figure 2 shows the hierarchical lamellar structure obtained from the self-assembly of $C'RCR'$ copolymers with $\chi N = 25$ and

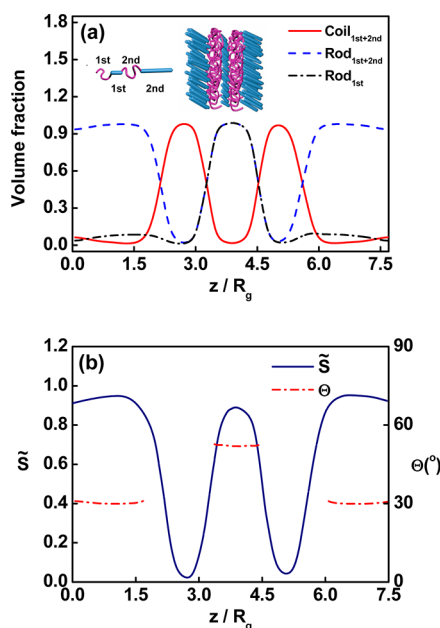


Figure 2. (a) One-dimensional density profiles of total coils ($Coil_{first+second}$), total rods ($Rod_{first+second}$), and short rod (Rod_{first}) of $C'RCR'$ multiblock copolymers with long R' end block; the volume fractions of each block are $f_{C'} = \Delta f_C = 0.15$, $\Delta f_R = 0.21$, and $f_{R'} = 0.49$. The insets show the schematic hierarchical smectic phases according to the density and order parameter profiles. (b) Order parameter \tilde{S} and averaged tilting angle Θ of rods within the domains of rods.

$f_{R'} = 0.49$. The volume fractions of R and C blocks are $f_{C'} = \Delta f_C = 0.15$ and $\Delta f_R = 0.21$. In Figure 2a, the density distributions of the total C and R blocks are displayed by red and blue lines. In order

to clarify the exact location of the different rod blocks, the density distribution of R midblocks (Rod_{first}) is also presented. As can be seen, the $C'RC$ part of $C'RCR'$ copolymers are microphase separated into three thin layers at the small length scale, where almost all the short R midblocks are distributed between two thin layers formed by $C(C')$ blocks. Meanwhile, the long R' end blocks form the large layers at the large length scale. The order parameter \tilde{S} and the average tilting angle Θ of rods as a function of position z along the layer normal \mathbf{n} are plotted in Figure 2b. As shown in Figure 2b, the order parameter (blue line) has a maximum value in the rod-rich regions, whereas the tilting degree of rods (red line) has different values in each rod domain. The higher values of order parameter ($\tilde{S} \approx 0.9$) in both the thin and thick rod-rich regions indicate that either the R midblocks or R' end blocks align perfectly. However, in individual domains, the tilting angles of rods are different, where $\Theta \approx 30^\circ$ and $\Theta \approx 50^\circ$ for long R' end blocks and short R midblocks. For the thick rod-rich region, the projected length of a rod block onto the layer normal can be calculated as $4.8R_g \times \cos(30^\circ) = 4.16R_g$, where the length of R' end block is $f_{R'} \times \beta = 4.8R_g$. This is nearly consistent with the domain size of the thick rod domains (about $4.18R_g$). Therefore, the large-length-scale structure is a monolayer S_C phase. For the thin rod-rich layers, the projected length of an R midblock is $1.22R_g$, which approaches the domain size of the thin layers (about $1.5R_g$). This implies that the small-length-scale structure is another S_C phase. We refer to such a hierarchical lamellar microstructure with two different-length-scale smectic phases as smectic-in-smectic (S_C -in- S_C) structures.

The stability of the observed hierarchical structures was further examined by comparing the free energies of other possible structures. By “seeding” lamellar initial structures for the SCFT, we can obtain various lamellae at different domain size D . Figure 3 shows the free energy of the obtained structures as a

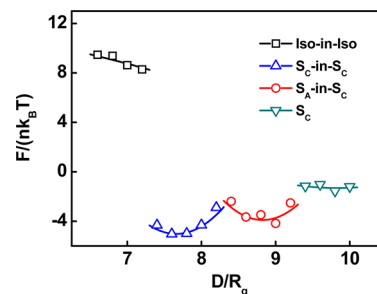


Figure 3. Free energy of various structures as a function of the domain size for $C'RCR'$ rod-coil multiblock copolymer at $\chi N = 25$. The global minimum corresponds to the S_C -in- S_C structures.

function of the domain size. The observed lamellar structures include smectic C phases (S_C), hierarchical structures with two isotropic phases (Iso-in-Iso), and hierarchical LC structures with two different-length-scale smectic phases (S_C -in- S_C and S_A -in- S_C). All the hierarchical structures have three internal layers at the small length scales. It can be seen that the S_C -in- S_C has the minimal free energy, indicating that it is the stable structure. On the other hand, the hierarchical structures with isotropic phases (not well-aligned rods) are the most unstable phase among these structures. From Figure 3, we noted that the free energy shows a dramatic decrease as the rod orientation changes from random alignment to ordered state. This means that the well alignment of the rod blocks is preferred for this system.

Since the alignment of rod blocks plays a key role in the formation of self-assembled structures, we further calculated the degree of rod alignment in different-length-scale layers as a function of interaction strength χN for C'RCR' with long R' end blocks. The result is presented in Figure 4a. When the χN values

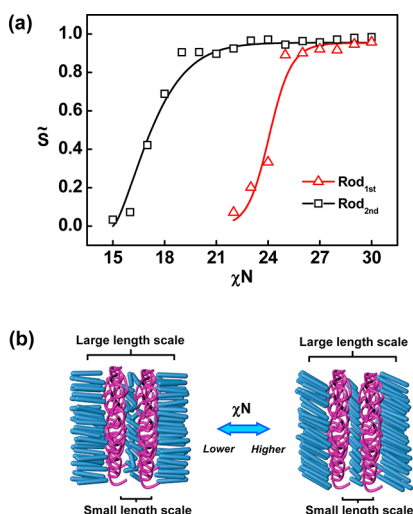


Figure 4. (a) Order parameter \tilde{S} of short rod (Rod_{first}) and long end rod (Rod_{second}) as a function of interaction strength χN for hierarchical smectic phases. The parameters are set the same as in Figure 2. (b) Schematic illustration of the phase transition between Iso-in-S_A and S_C-in-S_C with the variation of order parameter \tilde{S} .

are high enough, e.g., $\chi N > 25$, the order parameters of both the long R' and short R blocks are nearly identical ($\tilde{S} \approx 1$), indicating that the two kinds of rods are well aligned with each other. In such case, the hierarchical S_C-in-S_C structures have been observed (see Figure 2). With decreasing χN values, the order parameter of short R blocks becomes smaller until it approaches zero at about $\chi N = 21$. As $\chi N < 21$, the short R blocks form an isotropic structure in the thin rod-rich layers. However, the order parameter of long R' blocks still remains constant ($\tilde{S} \approx 0.08 - 0.9$). Meanwhile, the tilting angle becomes much smaller, which indicates that the rods are almost parallel to the lamella normal \mathbf{n} . Consequently, a hierarchical structure with isotropic and S_A phases (Iso-in-S_A) is formed. When the χN values are much smaller, the order parameter of the R' end blocks decreases dramatically. As a result, only the isotropic phases can be observed. It is of interest to find that the double periodic structures with different orientational orders are integrated in one system. The above phase transition between Iso-in-S_A and S_C-in-S_C as well as their possible chain arrangement has been schematically illustrated in Figure 4b. As shown in Figure 4b, in the case of lower interaction strength χN , the Iso-in-S_A phases with isotropic layers at small length scale and smectic lamellae at large length scale are observed. Once the χN value increases to some value, the short R blocks are well aligned to form the small-length-scale S_C phase, while the long R' end blocks arrange completely to form the large-length-scale S_C phase with some tilting angles.

In addition to the $n = 1$ cases, the $n = 2$ cases were also examined. Figure 5 shows the density profiles for the C'(RC)₂R' multiblock copolymers with $\chi N = 60$, $f_{R'} = 0.36$, $\Delta f_R = 0.12$, $f_{C'} = 0.24$, and $\Delta f_C = 0.08$. To clarify the detailed arrangement of rod segments, the density distributions of short R blocks (Rod_{first} and Rod_{second}) and long R' end blocks (Rod_{third}) are respectively

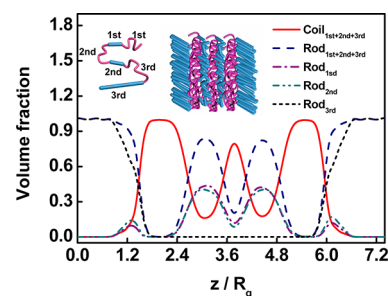


Figure 5. One-dimensional density profiles of total coils, total rods, short rods (Rod_{first} and Rod_{second}), and long end rod (Rod_{third}) of C'(RC)₂R' multiblock copolymers with $\chi N = 60$, $f_{R'} = 0.36$, $\Delta f_R = 0.12$, $f_{C'} = 0.24$, and $\Delta f_C = 0.08$. The insets show the schematic hierarchical smectic phases.

presented. As can be seen in Figure 5, the multiblock copolymers form a hierarchical LC lamellar structure, which consists of a large-length-scale smectic layer and a small-length-scale structure of two rod-containing and three coil-containing thin layers. The long R' end blocks are located in the thick smectic domains, while the short R blocks (Rod_{first} and Rod_{second}) are mostly distributed in the two thin LC layers. The order parameter \tilde{S} for the long and short rod blocks are respectively 0.992 and 0.390 (0.390 is the average order parameter of Rod_{first} and Rod_{second}), which implies that the long R' end blocks are well aligned but short R blocks are not. In addition, the tilting angle was calculated to determine the type of smectic structure of the long R' end blocks. In this case, the tilting angle is $\Theta \approx 50^\circ$. Based on the above analysis, an Iso-in-S_C phase with five inner layers was obtained. When the number of RC repeat units increases, more inner thin layers could be formed, due to the increase in possible molecular conformations. Moreover, the orientational order of short R blocks can be manipulated by changing the interaction strength χN . When the χN values become higher, the short R blocks can be aligned, and the smectic phase emerges at the small length scale. This variation trend is similar to that in Figure 4.

Notwithstanding the visual evidence of smectic-containing structure-in-structures, there remains a concern as to under which condition these structures exist. The length of rod blocks should play an important role. To deepen the understanding of the role played by the rod blocks in the hierarchical structure formation, we examined the effect of the relative length of rods, $l_{\text{first}}/(l_{\text{first}} + l_{\text{second}})$, where l_{first} and l_{second} are the lengths of short R midblock and the long R' end block, respectively. A typical result can be viewed from density variations of C'RCR' multiblock copolymers with $f_{R'} = \Delta f_R = 0.3$, $f_{C'} = \Delta f_C = 0.2$, and $\chi N = 25$, which is presented in Figure 6a. As can be seen, an asymmetric periodic lamellar phase has been observed, which contains thick rod-rich domains and thin coil-rich layers. It is noted that the volume fraction of the R midblocks is nearly half of that of the total rod blocks. This observation suggests that the R and R' blocks are intermixed with each other in the domains, which is different from the situation in Figure 4. To determine the detailed information of the structures, Figure 6b shows the degree \tilde{S} of the rod alignment and average tilting angle Θ of rods as a function of position z along the layer normal \mathbf{n} . In the rod-rich domains, the order parameter is almost unity, which implies that the rods are well-oriented. On the other hand, the tilting angle of rod blocks is quite small ($\Theta \approx 0^\circ$). Combining the results of \tilde{S} with Θ , we deduced that the complete alignments of these two intermixed rods result in the smectic A phase as the lengths of two rod blocks are comparable. Our further calculations reveal

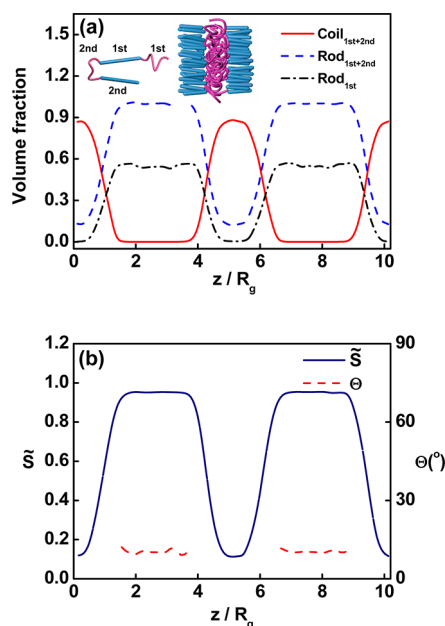


Figure 6. (a) One-dimensional density profiles of total coils, total rods, and middle rod ($\text{Rod}_{1\text{st}}$) of $\text{C}'\text{RCR}'$ multiblock copolymers with R' end block at equivalent relative rod length $l_{1\text{st}}/(l_{1\text{st}} + l_{2\text{nd}}) = 0.5$. The insets show the schematic smectic phases according to the density and order parameter profiles. (b) Order parameter \tilde{S} and averaged tilting angle Θ of rods within the domains of rods.

that the structure-in-structure with smectic phases appears only when the lengths of two rods are incomparable. Otherwise, the two rods can intermix with each other in one domain.

The above observation of different microstructures can be attributed to the difference in molecular arrangement in the rod-rich domains—whether the rod midblocks and end blocks are intermixed or not determines the ultimate self-assembled structures of $\text{C}'(\text{RC})_n\text{R}'$ multiblock copolymers. This reason can be directly explained by examining the period variation of the microstructures. Taking the $n = 1$ case as an example (herein, $\Delta f_{\text{C}} = f_{\text{C}'} = 0.2$), Figure 7 shows the period variation of

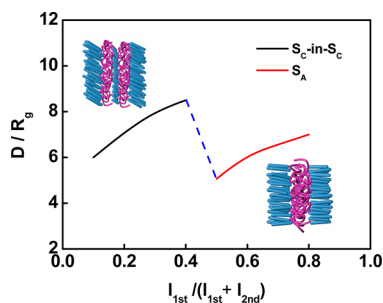


Figure 7. Equilibrium period D/R_g as a function of relative rod length $l_{1\text{st}}/(l_{1\text{st}} + l_{2\text{nd}})$ of $\text{C}'\text{RCR}'$ multiblock copolymers at $\Delta f_{\text{C}} = f_{\text{C}'} = 0.2$ and $\chi N = 25$. The insets represent the schematic of the phase transition from $\text{S}_{\text{C}}\text{-in-}\text{S}_{\text{C}}$ to smectic A corresponding to the variation of relative rod length.

the smectic phases as a function of relative length of different rods ($l_{1\text{st}}/(l_{1\text{st}} + l_{2\text{nd}})$). As shown in Figure 7, the overall period of the hierarchical smectic structures becomes larger with increasing the relative length $l_{1\text{st}}/(l_{1\text{st}} + l_{2\text{nd}})$. This results from not only the increase in the degree of separation between R midblocks and coil blocks but also the increase in the

orientational ordering of rod blocks in the small-length-scale domains of smectic-in-smectic structures. When the value of $l_{1\text{st}}/(l_{1\text{st}} + l_{2\text{nd}})$ is larger than 0.4, a dramatic decrease in the period occurs due to the fact that the R' and R blocks become intermixed. These results suggest that the increase in relative length of rod blocks leads to a phase transition from smectic-in-smectic structures to single-periodic smectic layers. From another viewpoint, the long R' end block plays a key role in formation of the rod-rich layer at the large length scale, which restricts the stretching of CRC multiblock units in small-length-scale domains. Once the lengths of the two blocks are almost equivalent, this constraint imposed by the thick domains formed by the R' end blocks vanishes suddenly. The R' and R blocks become intermixed and the corresponding structures are schemed in the insets of Figure 7.

2. Hierarchical Smectic Structures Self-Assembled from $\text{C}'(\text{RC})_n\text{R}'$ with Long C' End Block. In addition to the lengths of rod blocks, the hierarchical lamellar structures can be manipulated by changing the relative length of coil blocks in the $\text{C}'(\text{RC})_n\text{R}'$ multiblock copolymer system. In the study of the effect of coil blocks, we assumed that the C' end blocks are much longer than the R' end blocks. The value of the interaction strength is $\chi N/n = 25$, and the number of RC units is chosen as $n = 1$ or $n = 2$, respectively. Figure 8 shows the density profiles of total coil and rod blocks as a function of position z along the layer normal \mathbf{n} . As can be seen from Figure 8a, the $\text{C}'\text{RCR}'$ multiblock copolymers with $f_{\text{C}'} = 0.49$, $\Delta f_{\text{C}} = 0.21$, and $f_{\text{R}'} = \Delta f_{\text{R}} = 0.15$ self-assemble into an asymmetric layered structure, where the coil and rod blocks form the large and thin layers, respectively. The order parameter \tilde{S} of rod blocks is relatively small ($\tilde{S} = 0.032$), which implies that the rods are not oriented. In this case, the microphase separation of RCR' blocks for further generating small-length-scale structure does not take place.

We further examined the effect of n . Figure 8b shows a representative self-assembled structure of $\text{C}'(\text{RC})_2\text{R}'$ multiblock copolymers with $f_{\text{C}'} = 0.4$, $\Delta f_{\text{C}} = 0.15$, and $\Delta f_{\text{R}} = f_{\text{R}'} = 0.10$. The structure is hierarchical, which contains one thick amorphous layer formed by C blocks and three thin RCR' layers. Moreover, in terms of the results of orientational order parameter $\tilde{S} = 0.851$ in the rod-rich layers, the rod blocks could be well oriented. Such hierarchical lamellar structure possesses a smectic phase at the small length scale and an amorphous phase at the large length scale, and we therefore denoted it as S-in-A structure, where the S and A respectively represent the smectic and amorphous phases.

In this work, we observed two kinds of hierarchical structures, i.e., lamellae-in-lamella with one or two small-length-scale smectic phases. Of particular interest is the structure with two small-length-scale LC phases. Creation of hierarchical structures with LC characters has attracted attention in some recent studies. Ikkala et al. have produced double smectic structures in the solid state involving alternating layers of different polypeptide α -helices, self-assembled from ionically complexing di-*n*-butyl phosphate to poly(γ -benzyl-L-glutamate)-*b*-poly(L-lysine).⁵⁰ Hayakawa et al. have fabricated hierarchical LC structures from the self-assembly of double liquid crystalline side-chain-type block copolymers.⁵¹ In these structures, two kinds of semicrystalline side chains are oriented parallel to the interface of the microphase-separated lamellar structures. Chen et al. have created hierarchical structures with biaxial orientation via the self-assembly of a combined main-chain/side-chain liquid-crystalline polymer obtained by radical polymerization of a 2-vinylterephthalate,

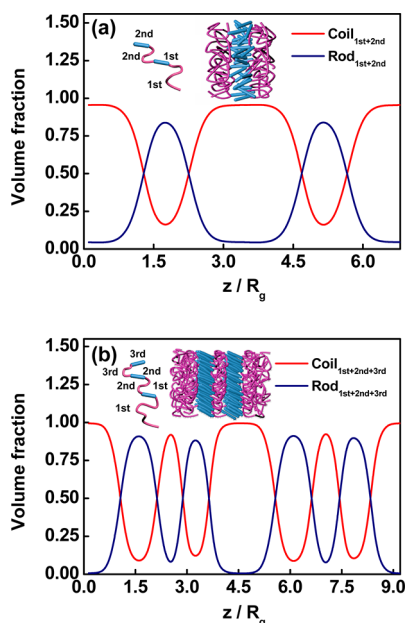


Figure 8. One-dimensional density profiles of total coils and rods of $C'(RC)_nR'$ multiblock copolymers with long C' end block at different number n of repeating units: (a) $n = 1$ and (b) $n = 2$. The insets show the schematic illustration of corresponding phases.

poly(2,5-bis[[6-(4-butoxy-4'-oxybiphenyl)hexyl]oxycarbonyl]-styrene).³² The side chains fill the space between the main chains, forming a smectic E structure with the side-chain axis perpendicular to that of the main chain. Note that, in these studies, the strategy for creating the hierarchical structures with double LC phases is to incorporate two kinds of chemically different liquid crystalline molecules. In contrast with these studies, we propose an alternative route to create hierarchical LC structures. In this route, the hierarchical smectic structures are formed from the self-assembly of the copolymers with only one type of liquid crystalline polymers but various lengths of the blocks, e.g., $C'(RC)_nR'$ multiblock copolymers with different lengths of rod blocks.

The hierarchical self-assembly behavior of the $C'(RC)_nR'$ multiblock copolymers can be further understood through comparing the present results with those obtained for flexible $A(BA)_nBA$ linear multiblock copolymers. For the $A(BA)_nBA$ multiblock copolymers, two important factors play important roles in determining the hierarchical structures: one is the number n of repeating units and the other is interaction strength χN .^{53,54} The studies have demonstrated that large values of n or χN are required for creating hierarchical structures such as lamellae-in-lamella. From this viewpoint, we initially deduced that large n and χN values are necessary for the $C'(RC)_nR'$ multiblock copolymers to form hierarchical structures. However, in actual calculations, we found that, in the rod-coil multiblock copolymer system, moderate interaction and fewer repeating units (herein, $\chi N = 50$ and $n = 2$) are sufficient to induce microphase separation between R and C midblocks to form small-length-scale structures, different from flexible copolymer systems. This can be attributed to the fact that the rod blocks are covalently linked to the flexible coils, and the low entropy of the rod blocks induces an easier separation between rod and coil blocks than that between coil and coil blocks. As a result, it is able to produce hierarchical structures at small values of n or χN in $C'(RC)_nR'$ copolymer melts, as compared with the flexible

$A(BA)_nBA$ copolymers. Moreover, the mismatch of the R and R' block lengths can enable the $C'(RC)_nR'$ multiblock copolymers to self-assemble into hierarchical LC structures. The aforementioned features are helpful for experimental preparation of hierarchical structures, since the lower molecular weight and less repeating blocks are favored for chemical synthesis.

The important feature of the hierarchical smectic structures is that they combine the orientational ordering properties of the LC systems and the rubber elasticity of the polymer domains (through suitable cross-linking of the coil blocks). The materials with such structures may perform as LC elastomers.^{55,56} The LC elastomers can be contracted under external stimuli such as heating, due to the nematic-to-isotropic phase transitions. Different from the conventional LC elastomers, the present materials can have distinct properties. As shown in Figure 4a, the two different-length-scale smectic phases have different responses to the interaction strength (the responses could be hierarchical). As a result, the materials fabricated by these copolymers could be contracted twice as the temperature varies. These double-stimuli-response materials can be used as muscle-like materials, based on the ideas proposed by de Gennes.⁵⁷ Since multiple stimuli responses are necessary for human-made materials, the materials produced by the present systems may find many advantages over the conventional LC elastomers.

CONCLUSION

We extended real-space self-consistent field theory to explore the hierarchical microstructures formed by $C'(RC)_nR'$ multiblock copolymers. Lamellae-in-lamella structures with double smectic phases, such as Iso-in- S_A and S_C -in- S_C structures, were observed in the self-assembly of $C'RCCR'$ tetrablock copolymers with longer R' end blocks (relative to C' blocks). It was found that these hierarchical smectic structures exhibit not only double periodicities in overall structure but also double orientational orders of rod blocks. The phase transition from Iso-in- S_A to S_C -in- S_C , with the change of the interaction strength, reflects the distinct feature in response to χN . Moreover, the S-in-A structures can be tailored by tuning the relative length of coil blocks. For the $C'(RC)_nR'$ multiblock copolymers with a longer C' end blocks, the hierarchical structures with one-length-scale smectic phase are formed. We anticipate that the present work could be helpful for the future design of hierarchical microstructures from copolymers.

AUTHOR INFORMATION

Corresponding Author

*Tel.: +86-21-64253370. E-mail: jlin@ecust.edu.cn.

Notes

The authors declare no competing financial interest.

ACKNOWLEDGMENTS

This work was supported by National Natural Science Foundation of China (50925308, 21234002), Key Grant Project of Ministry of Education (313020), and National Basic Research Program of China (No. 2012CB933600). Support from project of Shanghai municipality (10GG15) is also appreciated.

REFERENCES

- (1) Zvelindovsky, A. V. *Nanostructured Soft Matter: Experiments, Theory, Simulation and Perspectives*; Springer Verlag: Bristol, UK, 2007.
- (2) Tschierske, C. Micro-Segregation, Molecular Shape and Molecular Topology—Partners for The Design of Liquid Crystalline Materials with

Complex Mesophase Morphologies. *J. Mater. Chem.* **2001**, *11*, 2647–2671.

(3) Muthukumar, M.; Ober, C. K.; Thomas, E. L. Competing Interactions and Levels of Ordering in Self-Organizing Polymeric Materials. *Science* **1997**, *277*, 1225–1232.

(4) Hamley, I. W. *The Physics of Block Copolymers*; Oxford University Press: Oxford, UK, 1998.

(5) Lodge, T. P. Block Copolymers: Past Successes and Future Challenges. *Macromol. Chem. Phys.* **2003**, *204*, 265–273.

(6) Pitsikalis, M.; Pispas, S.; Mays, J. W.; Hadjichristidis, N. Nonlinear Block Copolymer Architectures. *Adv. Polym. Sci.* **1998**, *135*, 1–137.

(7) Hadjichristidis, N.; Iatrou, H.; Pitsikalis, M.; Pispas, S.; Avgeropoulos, A. Linear and Non-Linear Triblock Terpolymers. Synthesis, Self-Assembly in Selective Solvents and in Bulk. *Prog. Polym. Sci.* **2005**, *30*, 725–782.

(8) Tung, S. H.; Kalarickal, N. C.; Mays, J. W.; Xu, T. Hierarchical Assemblies of Block-Copolymer-Based Supramolecules in Thin Films. *Macromolecules* **2008**, *41*, 6453–6462.

(9) Lee, M.; Cho, B. K.; Zin, W. C. Supramolecular Structures From Rod-Coil Block Copolymers. *Chem. Rev.* **2001**, *101*, 3869–3892.

(10) Chen, J. T.; Thomas, E. L.; Ober, C. K.; Mao, G. Self-Assembled Smectic Phases in Rod-Coil Block-Copolymers. *Science* **1996**, *273*, 343–346.

(11) Thomas, E. L.; Chen, J. T.; O'Rourke, M. J. E.; Ober, C. K.; Mao, G. Influence of a Liquid Crystalline Block on the Microdomain Structure of Block Copolymers. *Macromol. Symp.* **1997**, *117*, 241–256.

(12) Tu, H.; Wan, X.; Liu, Y.; Chen, X.; Zhang, D.; Zhou, Q.-F.; Shen, Z.; Jason, J. G.; Jin, S.; Cheng, S. Z. D. Self-Assembly-Induced Supramolecular Hexagonal Columnar Liquid Crystalline Phase Using Laterally Attached Nonmesogenic Templates. *Macromolecules* **2000**, *33*, 6315–6320.

(13) Li, C. Y.; Tenneti, K. K.; Zhang, D.; Zhang, H.; Wan, X.; Chen, E.-Q.; Zhou, Q.-F.; Carlos, A.-O.; Igos, S.; Hsiao, B. S. Hierarchical Assembly of a Series of Rod-Coil Block Copolymers: Supramolecular LC Phase in Nanoenvironment. *Macromolecules* **2004**, *37*, 2854–2860.

(14) Tenneti, K. K.; Chen, X.; Li, C. Y.; Tu, Y.; Wan, X.; Zhou, Q.-F.; Sics, I.; Hsiao, B. S. Perforated Layer Structures in Liquid Crystalline Rod-Coil Block Copolymers. *J. Am. Chem. Soc.* **2005**, *127*, 15481–15490.

(15) Tenneti, K. K.; Chen, X.; Li, C. Y.; Wan, X.; Fan, X.; Zhou, Q.-F.; Rong, L.; Hsiao, B. S. Competition Between Liquid Crystallinity and Block Copolymer Self-assembly in Core-shell Rod-coil Block Copolymers. *Soft Matter* **2008**, *4*, 458–461.

(16) Chen, X. F.; Shen, Z.; Wan, X. H.; Fan, X. H.; Chen, E.-Q.; Ma, Y.; Zhou, Q.-F. Mesogen-jacketed Liquid Crystalline Polymers. *Chem. Soc. Rev.* **2010**, *39*, 3072–3101.

(17) Ikkala, O.; ten Brinke, G. Functional Materials Based on Self-Assembly of Polymeric Supramolecules. *Science* **2002**, *295*, 2407–2409.

(18) Ruokolainen, J.; ten Brinke, G.; Ikkala, O. Supramolecular Polymeric Materials with Hierarchical Structure-within-Structure Morphologies. *Adv. Mater.* **1999**, *11*, 777–780.

(19) Valkama, S.; Kosonen, H.; Ruokolainen, J.; Haatainen, T.; Torkkeli, M.; Serimaa, R.; ten Brinke, G.; Ikkala, O. Self-assembled Polymeric Solid Films with Temperature-Induced Large and Reversible Photonic-Bandgap Switching. *Nat. Mater.* **2004**, *3*, 872–876.

(20) Ruotsalainen, T.; Turku, J.; Heikkilä, P.; Ruokolainen, J.; Nykänen, A.; Laitinen, T.; Torkkeli, M.; Serimaa, R.; ten Brinke, G.; Harlin, A. Towards Internal Structuring of Electrospun Fibers by Hierarchical Self-Assembly of Polymeric Comb-Shaped Supramolecules. *Adv. Mater.* **2005**, *17*, 1048–1052.

(21) Matsushita, Y. Precise Molecular Design of Complex Polymers and Morphology Control of Their Hierarchical Multiphase Structures. *Polym. J.* **2008**, *40*, 177–183.

(22) Matsushita, Y.; Takano, A.; Hayashida, K.; Asari, T.; Noro, A. Hierarchical Nanophase-Separated Structures Created by Precisely-Designed Polymers with Complexity. *Polymer* **2009**, *50*, 2191–2203.

(23) Masuda, J.; Takano, A.; Suzuki, J.; Nagata, Y.; Noro, A.; Hayashida, K.; Matsushita, Y. Composition-Dependent Morphological

Transition of Hierarchically-Ordered Structures Formed by Multiblock Terpolymers. *Macromolecules* **2007**, *40*, 4023–4027.

(24) Matsushita, Y. Creation of Hierarchically Ordered Nanophase Structures in Block Polymers Having Various Competing Interactions. *Macromolecules* **2007**, *40*, 771–776.

(25) Potemkin, I. I.; Bodrova, A. S. A Theory of Microphase Separation in the Melt of Diblock Copolymers with Smectic Liquid Crystalline Side Groups. *Macromolecules* **2009**, *42*, 2817–2825.

(26) Junnila, S.; Houbenov, N.; Hanski, S.; Iatrou, H.; Hirao, A.; Hadjichristidis, N.; Ikkala, O. Hierarchical Smectic Self-Assembly of an ABC Miktoarm Star Terpolymer with a Helical Polypeptide Arm. *Macromolecules* **2010**, *43*, 9071–9076.

(27) Hamley, I. W. *Introduction to Soft Matter: Polymers, Colloids, Amphiphiles and Liquid Crystals*; John Wiley & Sons Ltd: Chichester, UK, 2000.

(28) Dervichian, D. G. The Control of Lyotropic Liquid-Crystals, Biological and Medical Implications. *Mol. Cryst. Liq. Cryst.* **1977**, *40*, 19–31.

(29) Hsu, C.-S. The Application of Side-Chain Liquid-Crystalline Polymers. *Prog. Polym. Sci.* **1997**, *22*, 829–871.

(30) Haataja, J. S.; Houbenov, N.; Iatrou, H.; Hadjichristidis, N.; Karatzas, A.; Faul, C. F. J.; Rannou, P.; Ikkala, O. Double Smectic Self-Assembly in Block Copolypeptide Complexes. *Biomacromolecules* **2012**, *13*, 3572–3580.

(31) Maeda, R.; Hayakawa, T.; Tokita, M.; Kikuchi, R.; Kouki, J.; Kakimoto, M.; Urushibata, H. Double Liquid Crystalline Side-Chain Type Block Copolymers for Hierarchically Ordered Nanostructures: Synthesis and Morphologies in the Bulk and Thin Film. *React. Funct. Polym.* **2009**, *69*, 519–529.

(32) Xie, H.-L.; Jie, C.-K.; Yu, Z.-Q.; Liu, X.-B.; Zhang, H.-L.; Shen, Z.; Chen, E.-Q.; Zhou, Q.-F. Hierarchical Supramolecular Ordering with Biaxial Orientation of a Combined Main-Chain/Side-Chain Liquid-Crystalline Polymer Obtained from Radical Polymerization of 2-Vinylterephthalate. *J. Am. Chem. Soc.* **2010**, *132*, 8071–8080.

(33) Matsen, M. W.; Barrett, C. Liquid-Crystalline Behavior of Rod-Coil Diblock Copolymers. *J. Chem. Phys.* **1998**, *109*, 4108–4119.

(34) Shah, M.; Pryamitsyn, V.; Ganesan, V. A Model for Self-Assembly in Side Chain Liquid Crystalline Block Copolymers. *Macromolecules* **2008**, *41*, 218–229.

(35) Shah, M.; Ganesan, V. Correlations between Morphologies and Photovoltaic Properties of Rod-Coil Block Copolymers. *Macromolecules* **2010**, *43*, 543–552.

(36) Pryamitsyn, V.; Ganesan, V. Self-Assembly of Rod-Coil Block Copolymers. *J. Chem. Phys.* **2004**, *120*, 5824–5838.

(37) Matsen, M. W. Melts of Semiflexible Diblock Copolymer. *J. Chem. Phys.* **1996**, *104*, 7758–7764.

(38) Shah, M.; Ganesan, V. Chain Bridging in a Model of Semicrystalline Multiblock Copolymers. *J. Chem. Phys.* **2009**, *130*, 054904.

(39) Chen, J. Z.; Zhang, C. X.; Sun, Z. Y.; Zheng, Y. S.; An, L. J. A Novel Self-Consistent-Field Lattice Model for Block Copolymers. *J. Chem. Phys.* **2006**, *124*, 104907.

(40) Xia, Y.; Chen, J.; Sun, Z.; Shi, T.; An, L.; Jia, Y. Self-Assembly of T-Shaped Rod-Coil Block Copolymer Melts. *J. Chem. Phys.* **2009**, *131*, 144905.

(41) Wang, L.; Lin, J.; Zhang, L. Hierarchically Ordered Microstructures Self-Assembled from A(BC)_n Multiblock Copolymers. *Macromolecules* **2010**, *43*, 1602–1609.

(42) Zhu, X.; Wang, L.; Lin, J.; Zhang, L. Ordered Nanostructures Self-Assembled from Block Copolymer Tethered Nanoparticles. *ACS Nano* **2010**, *4*, 4979–4988.

(43) Zhang, L.; Lin, J. Hierarchically Ordered Nanocomposites Self-Assembled from Linear-Alternating Block Copolymer/Nanoparticle Mixture. *Macromolecules* **2009**, *42*, 1410–1414.

(44) Tao, Y.; Olsen, B. D.; Ganesan, V.; Segalman, R. A. Domain Size Control in Self-Assembling Rod-Coil Block Copolymer and Homopolymer Blends. *Macromolecules* **2007**, *40*, 3320–3327.

(45) Fredrickson, G. H. *The Equilibrium Theory of Inhomogeneous Polymers*; Oxford University Press: Oxford, UK, 2006.

- (46) Drolet, F.; Fredrickson, G. H. Combinatorial Screening of Complex Block Copolymer Assembly with Self-Consistent Field Theory. *Phys. Rev. Lett.* **1999**, *83*, 4317–4320.
- (47) Ganesan, V.; Fredrickson, G. H. Field-theoretic Polymer Simulations. *Europhys. Lett.* **2001**, *55*, 814–820.
- (48) Drolet, F.; Fredrickson, G. H. Optimizing Chain Bridging in Complex Block Copolymers. *Macromolecules* **2001**, *34*, 5317–5324.
- (49) Tzeremes, G.; Rasmussen, K. Ø.; Lookman, T.; Saxena, A. Efficient Computation of the Structural Phase Behavior of Block Copolymers. *Phys. Rev. E* **2002**, *65*, 041806.
- (50) Rasmussen, K. Ø.; Kalsakas, G. Improved Numerical Algorithm for Exploring Copolymer Mesophases. *J. Polym. Sci., Part B: Polym. Phys.* **2002**, *40*, 1777–1783.
- (51) Eyert, V. A Comparative Study on Methods for Convergence Acceleration of Iterative Vector Sequences. *J. Comput. Phys.* **1996**, *124*, 271–285.
- (52) Bohbot-Raviv, Y.; Wang, Z. G. Discovering New Ordered Phases of Block Copolymers. *Phys. Rev. Lett.* **2000**, *85*, 3428–3431.
- (53) Nap, R.; Sushko, N.; Erukhimovich, I.; ten Brinke, G. Double Periodic Lamellar-in-Lamellar Structure in Multiblock Copolymer Melts with Competing Length Scales. *Macromolecules* **2006**, *39*, 6765–6770.
- (54) Nagata, Y.; Masuda, J.; Noro, A.; Cho, D.; Takano, A.; Matsushita, Y. Preparation and Characterization of a Styrene-Isoprene Undecablock Copolymer and Its Hierarchical Microdomain Structure in Bulk. *Macromolecules* **2005**, *38*, 10220–10225.
- (55) Li, M. H.; Keller, P.; Yang, J.; Albouy, P. A. An Artificial Muscle with Lamellar Structure Based on a Nematic Triblock Copolymer. *Adv. Mater.* **2004**, *16*, 1922–1925.
- (56) Li, M. H.; Keller, P. Artificial Muscles Based on Liquid Crystal Elastomers. *Philos. Trans. R. Soc. A* **2006**, *364*, 2763–2777.
- (57) de Gennes, P. G.; Hébert, M.; Kant, R. Artificial Muscles Based on Nematic Gels. *Macromol. Symp.* **1997**, *113*, 39–49.